

Supporting information for

**FRET-based colorimetric and ratiometric fluorescent probe
for Cu²⁺ with a new trimethylindolin fluorophore**

Jiao Zhang,^a Mei Zhu,^b Daoyong Jiang,^a Han Zhang,^a Luying Li,^a Guoning Zhang,^b
Yucheng Wang,^b Chao Feng,^c Hong Zhao*^a

^a School of Chemistry and Chemical Engineering, Southeast University, Nanjing,
211189, China

^b Institute of Medicinal Biotechnology, Chinese Academy of Medical Sciences and
Peking Union Medical College, Beijing, 100050, China

^c School of Materials and Chemical Engineering, Bengbu University, Bengbu 233030,
P. R. China

* Corresponding author E-mail address: zhaohong@seu.edu.cn

Contents

Fig. S1 The overlap (shown with oblique stripes) between emission of the donor and absorption spectra of the acceptor.

Fig. S2 A plot of absorbance of **RhF** against Cu^{2+} (0- 120 μM).

Fig. S3 A plot of Bensei-Hildebrand obtained from the UV-Vis absorption.

Fig. S4 Changes of the fluorescence spectra of **RhF** (10 μM) observed upon addition of various metal ions in a CH_3CN /aqueous HEPES buffer (10 mM, pH 7.3; 4:1, v/v).

Fig. S5 Calculations for FRET efficiency.

Fig. S6 Fluorescence titration spectra of **RhF** (10 μM) in the presence of different concentrations of Cu^{2+} (0-50 μM).

Fig. S7 The plot of the emission intensity ratios of **RhF** at I582/I503 against Cu^{2+} (88-140 μM).

Fig. S8 Effect of pH on probe for the detection of Cu^{2+} .

Fig. S9 The changes of fluorescence intensity at 503 nm of probe **RhF** exposed to light for a long time.

Fig. S10 Job's plot of probe **RhF** with Cu^{2+} in a CH_3CN /aqueous HEPES buffer (10 mM, pH=7.3; 4:1 v/v).

Fig. S11 ESI-MS spectrum of probe **RhF-Cu²⁺** complex.

Fig. S12 ^1H NMR spectra of **RhF-Cu²⁺** (a) in DMSO-d_6 with D_2O and **RhF** (b) in DMSO-d_6 .

Fig. S13. XPS of as prepared samples: (A) survey spectra of **RhF-Cu²⁺** complex; (B) $\text{Cu}2\text{p}$ of **RhF-Cu²⁺** complex.

Fig. S14 IR spectral data of **RhF** and **RhF-Cu²⁺** complex.

Fig. S15 Effect of water content on probe for the detection of Cu^{2+} .

Fig. S16 ESI-MS spectrum of probe **RhF**.

Fig. S17 ^1H NMR Spectrum of probe **RhF**.

Fig. S18 ^{13}C NMR Spectrum of probe **RhF**.

Table S1 Comparison of the recently reported probes for the detection of Cu^{2+} .

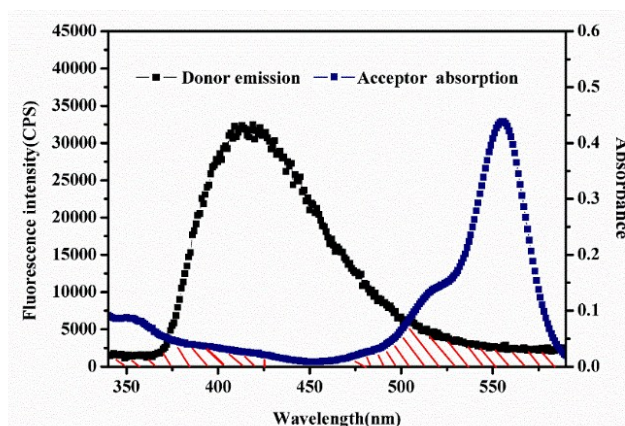


Fig. S1 The overlap (shown with oblique stripes) between emission of the donor and absorption spectra of the acceptor, respectively.

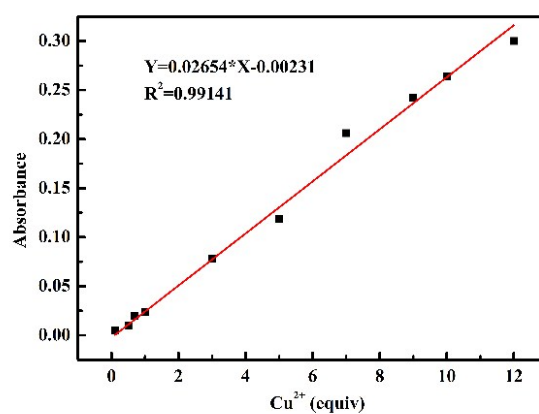


Fig. S2 Absorbance plot of **RhF** against Cu²⁺ concentration from 0 to 120 μ M.

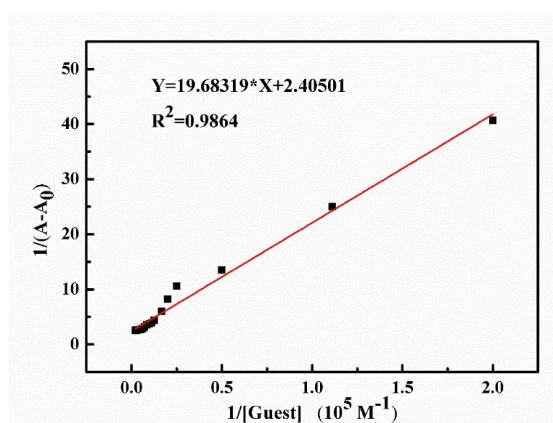


Fig. S3 Bensei-Hildebrand plot of **RhF-Cu²⁺** complex obtained from the UV-Vis absorption (absorbance calculated from 555 nm) studies.

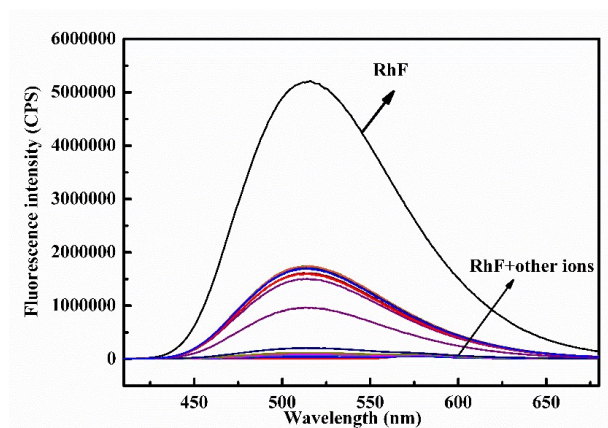


Fig. S4 Changes of the fluorescence spectra of **RhF** (10 μ M) observed upon addition of various metal ions in a CH₃CN/aqueous HEPES buffer (10 mM, pH 7.3; 4:1, v/v).

Fig. S5 Calculations for FRET efficiency:

Energy transfer efficiency (Φ_{ET}) was evaluated through the following equation: ¹⁻⁴

$$\Phi_{ET} = 1 - (F'_D / F)$$

where F'_D and F_D denote the donor fluorescence intensity with and without an acceptor respectively in the presence of Cu²⁺ ions.

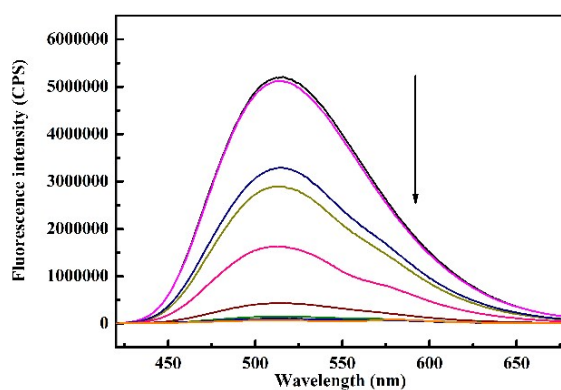


Fig. S6 Fluorescence titration spectra of **RhF** (10 μ M) in the presence of different concentrations of Cu²⁺ (0-50 μ M). λ_{exc} = 345 nm.

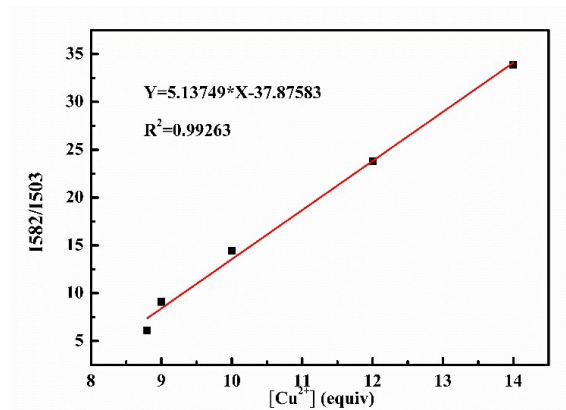


Fig. S7 The plot of the emission intensity ratios of **RhF** at I582/I503 against Cu²⁺ (88-140μM).

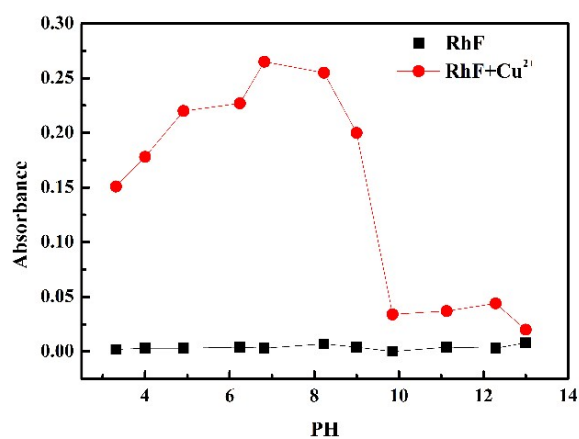


Fig. S8 Effect of pH on probe for the detection of Cu²⁺ (based on absorbance data).

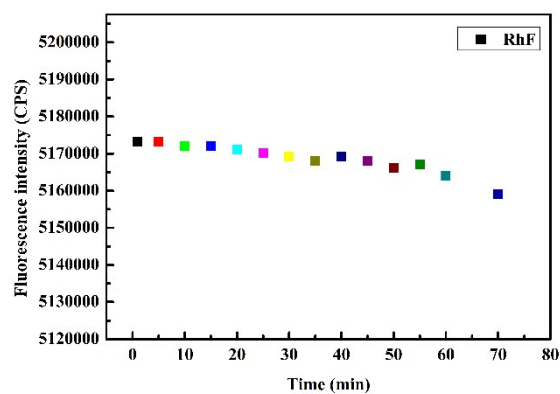


Fig. S9 The changes of fluorescence intensity at 503 nm of probe **RhF** exposed to light for a long time.

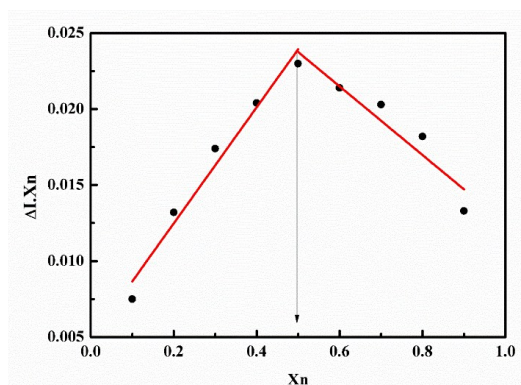


Fig. S10 Job's plot of probe **RhF** with Cu^{2+} in a CH_3CN /aqueous HEPES buffer (10 mM, pH=7.3; 4:1 v/v). Where X_n is the mole fraction of **RhF** and ΔI is the change ($I-I_0$) in the absorbance in presence of Cu^{2+} . The total concentration of RhF and Cu^{2+} was $20\mu\text{M}$.

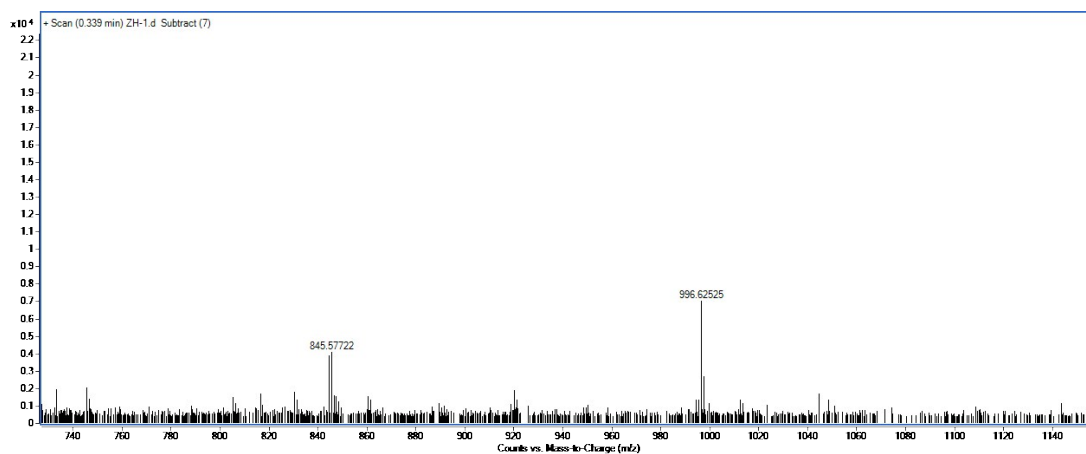


Fig. S11 ESI-MS spectrum of probe **RhF-Cu²⁺** complex.

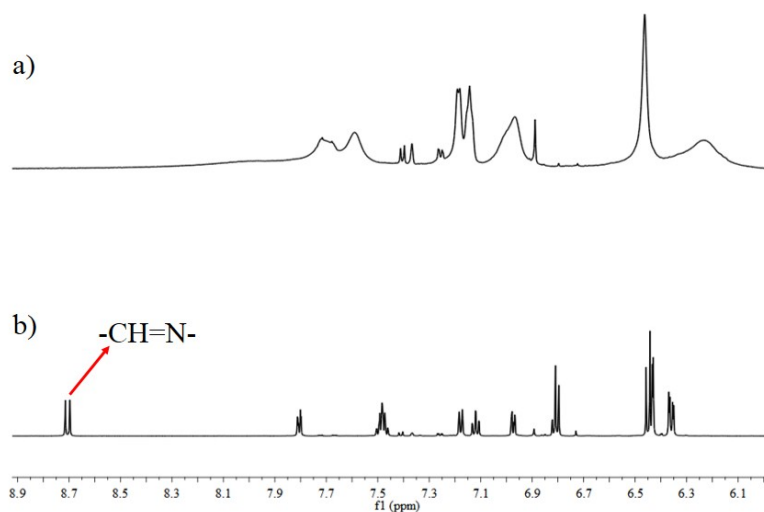


Fig.S12 ¹H NMR spectra of **RhF-Cu²⁺** (a) in DMSO-d_6 with D_2O and **RhF** (b) in DMSO-d_6 .

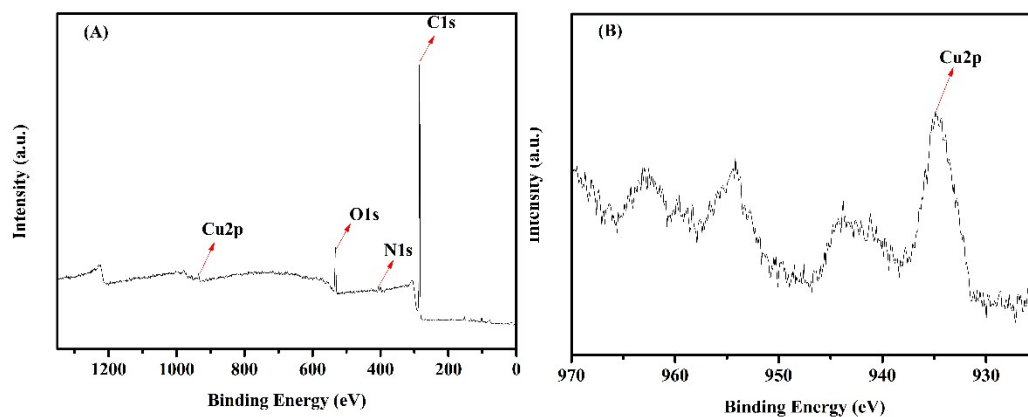


Fig. S13. XPS of as prepared samples: (A) survey spectra of RhF-Cu^{2+} complex; (B) Cu 2p of RhF-Cu^{2+} complex.

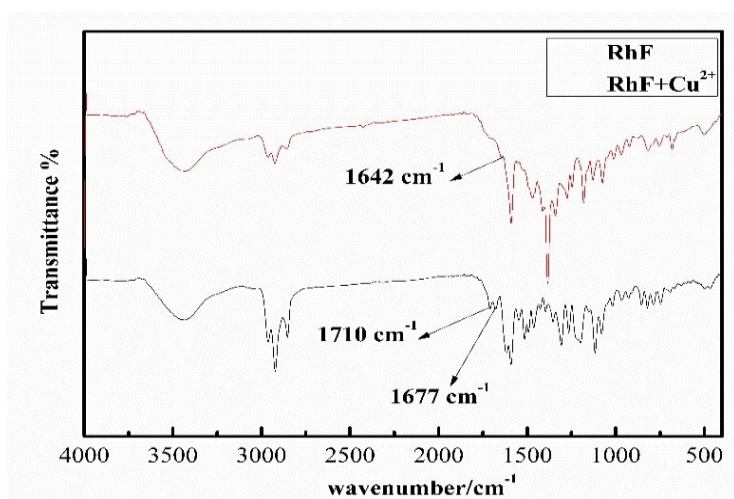


Fig.S14 IR spectral data of RhF and RhF-Cu^{2+} complex.

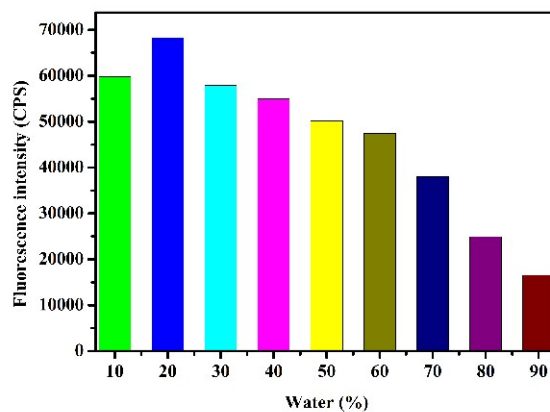


Fig. S15 Effect of water content on probe for the detection of Cu^{2+} .

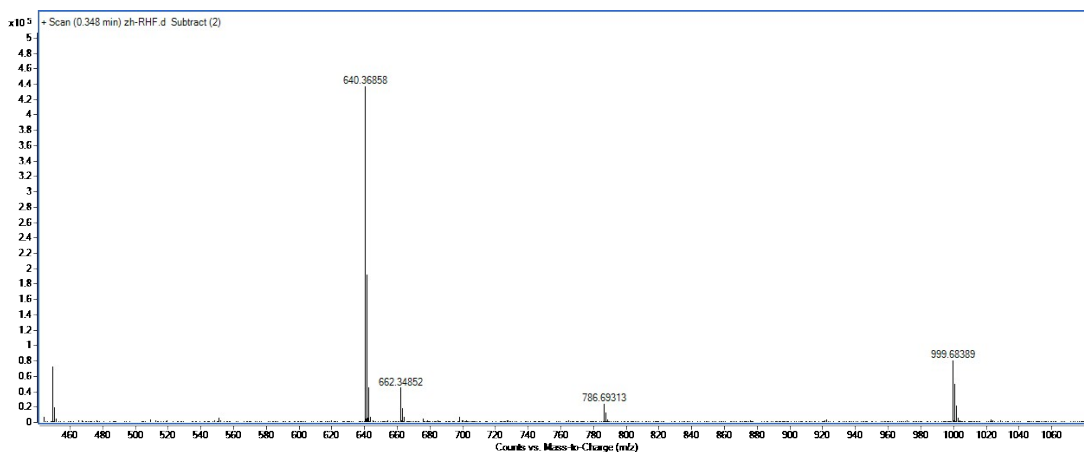


Fig. S16 ESI-MS spectrum of probe RhF.

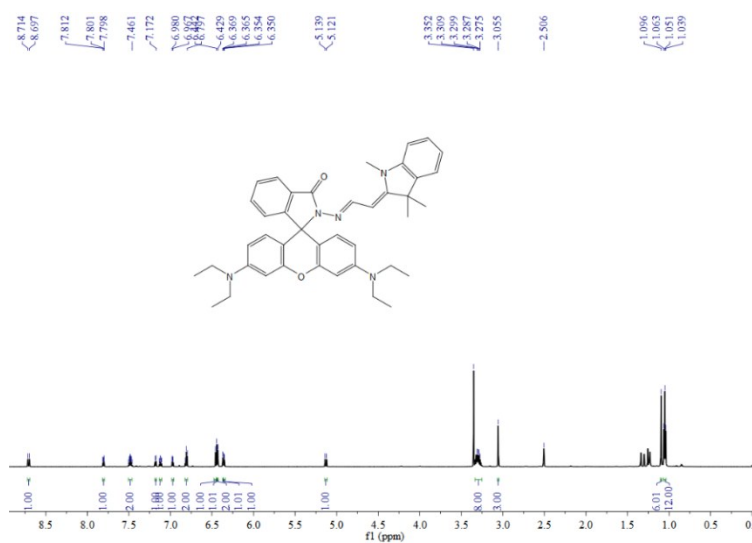


Fig. S17 ¹H NMR Spectrum of probe RhF.

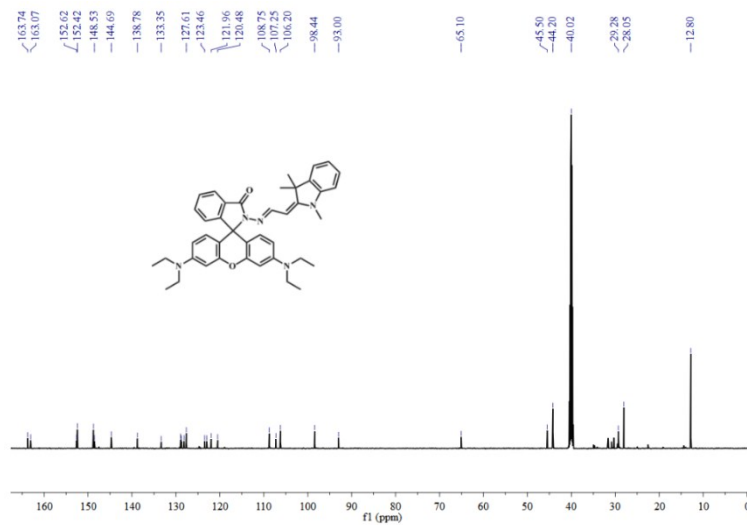
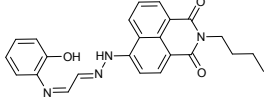
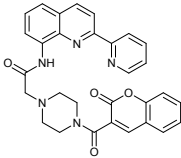
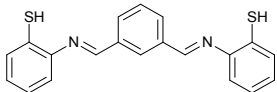
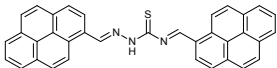
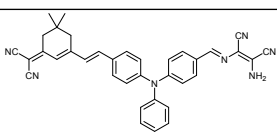
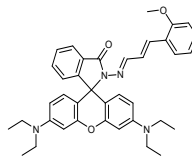
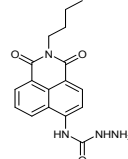
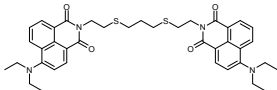
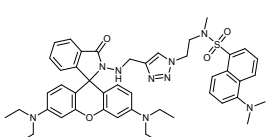
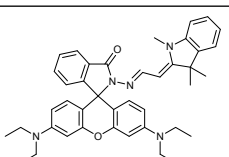


Fig. S18 ¹³C NMR Spectrum of probe RhF.

Table S1 Comparison of the recently reported probes for the detection of Cu²⁺.

Probes	$\lambda_{\text{ex}}/\lambda_{\text{em}}$ (nm)	Detection Limit (μM)	Working system	Operation mode	Analytical application: test strips	Ref.
	455/519	0.15	CH ₃ CN-H ₂ O (70:30, v/v, MOPS, 10 mM, pH = 7.0)	Turn-ON	NO	[5]
	290/ 355、 470	0.46	CH ₃ CN-H ₂ O(3:2, v/v,10 mM Tris- HCl)	Turn-OFF	NO	[6]
	295/365	0.2	CH ₃ CN-H ₂ O (2:3,v/v)	Turn-ON	NO	[7]
	376/439	14.5	CH ₃ CN	Turn-ON	NO	[8]
	437/637	1.568	CH ₃ CN	Turn-ON	NO	[9]
	None	0.29	CH ₃ CN	Turn-ON	NO	[10]
	435/532	0.052	CH ₃ CN-H ₂ O (20:80, v/v, pH=7.4)	Turn-ON	NO	[11]
	419/524	13.05	CH ₃ CN-H ₂ O (99:1, v/v)	Turn-ON	NO	[12]
	420/ 540、 568	0.12	CH ₃ CN-HEPES (1 : 1, v/v, 20 mM, pH= 7.4)	Turn-ON	No	[13]
	345/ 503、 582	0.01168	CH ₃ CN-aqueous HEPES buffer (4:1, v/v, 10 mM, PH=7.3)	Turn-ON	YES	This work

References

- 1 J. R. Lakowicz, *Topics in Fluorescence Spectroscopy Volume 2: Principles*, Kluwer Academic Publishers, New York, 2002.
- 2 D. Seth, A. Chakraborty, P. Setua, D. Chakrabarty, N. Sarkar, *The Journal of Physical Chemistry B*, 2005, 109, 12080-12085.
- 3 S. L. Gilat, A. Adronov, J. M. J. Fréchet, *Int. Ed. Angew. Chem., Int. Ed.* 1999, 38, 1422-1427.
- 4 M. H. Lee, D. T. Quang, H. S. Jung, J. Yoon, C.-H. Lee, J. S. Kim, *J. Org. Chem.* 2007, 72, 4242-4245.
- 5 Z. Chen, L. Wang, G. Zou, J. Tang, X. Cai, M. Teng and L. Chen, *Spectrochim Acta A Mol Biomol Spectrosc*, 2013, 105, 57-61.
- 6 Y. Zhang, X. Guo, X. Tian, A. Liu and L. Jia, *Sensors and Actuators B: Chemical*, 2015, 218, 37-41.
- 7 H. Diao, W. Niu, W. Liu, L. Feng and J. Xie, *Spectrochim Acta A Mol Biomol Spectrosc*, 2017, 170, 65-68.
- 8 S. Bayindir and M. Toprak, *Spectrochim Acta A Mol Biomol Spectrosc*, 2019, 213, 6-11.
- 9 W. Li, Y. Zhang, X. Gan, M. Yang, B. Mie, M. Fang, Q. Zhang, J. Yu, J. Wu, Y. Tian and H. Zhou, *Sensors and Actuators B: Chemical*, 2015, 206, 640-646.
- 10 Q. Hu, Y. Liu, Z. Li, R. Wen, Y. Gao, Y. Bei and Q. Zhu, *Tetrahedron Letters*, 2014, 55, 4912-4916.
- 11 X.-X. Hu, X.-L. Zheng, X.-X. Fan, Y.-T. Su, X.-Q. Zhan and H. Zheng, *Sensors and Actuators B: Chemical*, 2016, 227, 191-197.
- 12 S. Thavornpradit, J. Sirirak and N. Wanichacheva, *Journal of Photochemistry and Photobiology A: Chemistry*, 2016, 330, 55-63.
- 13 Z. Hu, J. Hu, Y. Cui, G. Wang, X. Zhang, K. Uvdal and H.-W. Gao, *Journal of Materials Chemistry B*, 2014, 2.